Electronic Supplementary Material (ESI) for Energy & Environmental Science

Supplementary Information

Conjunction of fiber solar cells with groovy micro-reflectors as highly efficient energy harvester

Yongping Fu, [1]Zhibin Lv, [1]Shaocong Hou,[1] Hongwei Wu, [1] Dang Wang, [1] Chao Zhang, [1] Zengze Chu, Xin Cai,[1] Xing Fan, [1] **Zhonglin Wang**, [*2] **Dechun Zou**[*1]

[1]*Beijing National Laboratory for Molecular Sciences, Key Laboratory of Polymer Chemistry and Physics of Ministry of Education, College of Chemistry and Molecular Engineering, Peking University, Beijing 100871*

Email: dczou@pku.edu.cn

[2] *School of Materials Science and Engineering, Georgia Institute of Technology, Atlanta, GA 30332-0245, USA*

E-mail: zhong.wang@mse.gatech.edu

Part 1, Current and power outputs of FPVs under the diffuse light model

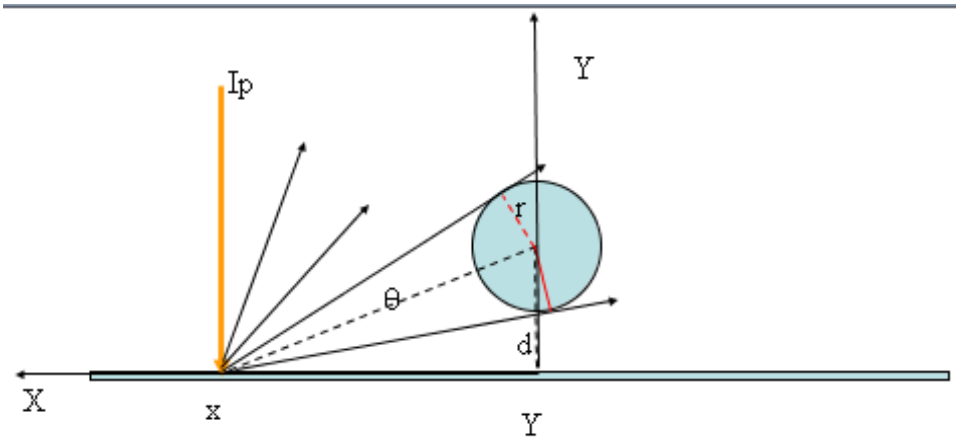

Fig. 1. Schematic of the diffuse reflection light model

A FPVC is located at the center of a diffuse plate, as seen in Fig. 1. Let its radius be r, the distance of the cell's center away from the diffuse plate is d. To simplify the

calculation, we assume:

1). Parallel incident light perpendicularly falls on the diffuse plate;

2). Diffuse light reflected from the diffuse plate is ideal diffuse light, there exists no mirror reflection of light from the plate, and no absorption and transmission in the plate;

3).The diffuse light intensity I_d follows Lambert's law of diffuse reflection. It is only direct proportional to the cosine of the angle ϕ between the incident light direction and the normal direction of the surface at the reflection point, that is,

$$I_d = I_0 \times K_d \times \cos\phi,$$

where I_0 is incident light intensity, K_d ($0 < K_d \leq 1$) is the surface diffuse reflection factor, ϕ is the angle mentioned above. In the condition of ideal diffuse reflection, $K_d = 1$, thus, the diffuse reflection intensity at a distance x from the cell is simplified as $I_d(x) = I_0 \times \cos\phi.$

4). Assuming that the short-circuit current is positively proportional to the diffuse light intensity.

Based on the above, only the part of diffuse reflection light in the angle θ at the diffuse reflection point (x, 0) on the plate can be collected by the fiber cell. Therefore, the ratio of it to total incident light intensity is defined as:

$$\psi = \frac{\int_{\theta_1}^{\theta_2} I_0 \cos\phi d\phi}{I_0}, \theta_2 - \theta_1 = \theta,$$

$$\theta_1 = \frac{\pi}{2} - 2\arcsin\frac{r}{\sqrt{x^2 + r^2}} - \arctan\frac{d-r}{r},$$

$$\theta_2 = \frac{\pi}{2} - \arctan\frac{d-r}{r},$$

$$\psi = \sin\theta_2 - \sin\theta_1$$

Then, the ratio of diffuse reflection light in the range from (-x, 0) to (x, 0) on the diffuse plate collected by the fiber cell to total incident light should be:

$$\psi(x) = 2\int_{-x}^{x}[\sin(\theta_2) - \sin(\theta_1)]dx,$$

According to assumption 4, the short-circuit current and power (directly proportional to the photoelectrical conversion efficiency) output by the cell due to diffuse reflection light is as follows:

$$J = J_0 \times (1 + \psi(x)),$$

$$P = P_0 \times (1 + \psi(x)),$$

where J_0 and P_0 are the short-circuit current and power output by the cell without the diffuse plate, respectively; and J and P are the short-circuit current and power output by the cell when the width of the diffuse plate is 2x, respectively.

Further we define a diffuse enhancement factor as follows:

$$\beta = K\frac{J}{J_0} = \frac{P}{P_0} = K(1 + \psi(x)).$$

It presents the cell's ability to utilize the diffuse plate, where K is a correction factor. The reasons to introduce K are (a) real diffuse reflection is not ideal; (b) the reflectivity of the cell's sealing tube to incident light at different incident angles are different. For ideal condition K=1.00. For real condition, we can adjust K value to correct the simulation results to fit well with the experiments data.

Simulation results in ideal condition are shown in figure 2. $\psi(x)$ decreases sharply with x increasing, which means that FPVC harvest less light coming away from itself. As a result, β will reach its limited value (limited β =2.05 shown in

figure 2) as x increase . For example, in figure 3, when K equals to 1.10, the simulation results agree well with experiments results.

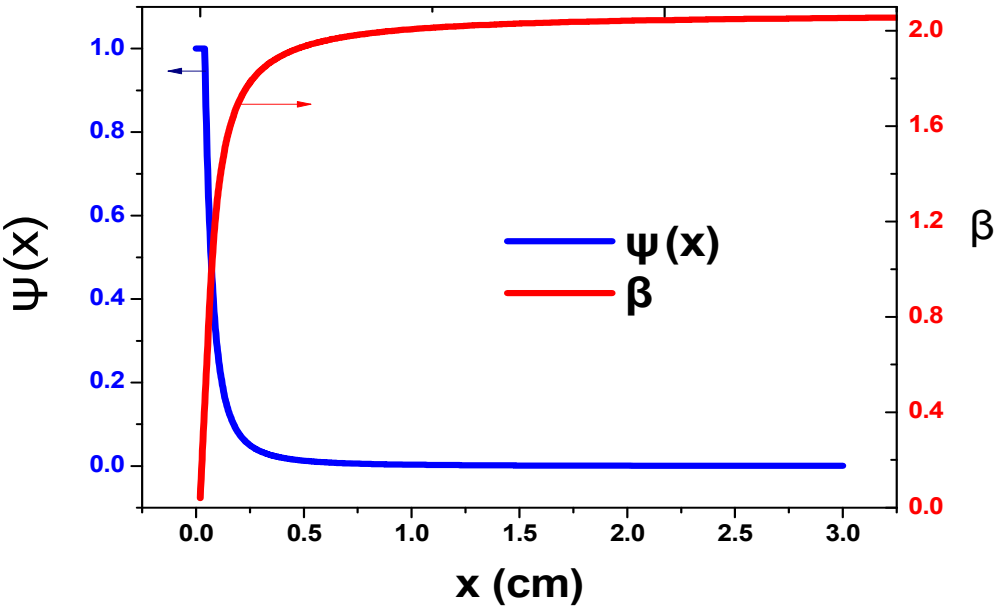

Fig. 2. Relationships of the ratio of the diffuse reflection light ψ(x), the diffuse reflection enhancement factor β to the half-width of the diffuse plate calculated when the cell's radius r = 0.4 cm and the diffuse plate is close to the cell (d = 0 mm).

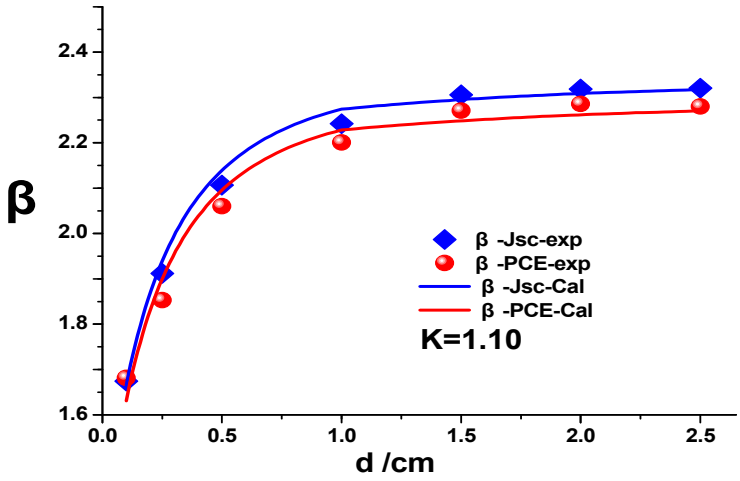

Fig. 3. The diffuse enhancement factor β as a function of the different diffuse plate half-width.

Part 2, Angle dependence

Solar cells were respectively spun around x-, y-, and z-axes to mimic the changes of the incident angles of daily sunlight, as shown in main text figure 3a and 3b.

For fiber solar Cell A, the short circuit current when FPVC rotates along with corresponding axes satisfies

$$J_{F,x} = J_{F,z} = J_0, J_{F,y} = K \times J_0 \times \cos\theta.$$

For fiber solar cell A with the diffuse plate underneath the devices, it satisfies

$$J_{F,x} = K \times J_0 \times (1 + \cos\theta), J_{F,y} = K \times J_0 \times \cos\theta, J_{F,Z} = J_0,$$

While for the planar Cell C, it satisfies

$$J_{P,x} = J_0, J_{P,z} = J_{P,y} = K \times J_0 \times \cos\theta,$$

where $J_{F,T}$ is the short circuit current in the corresponding coordinate, the sub-indicts F and P denote the fibrous cell A and the planar cell B. T stands for x, y, and z. θ is the incident angle of light and J_0 is the short circuit current when $\theta = 0$.

Part 3, fabrication of planar cell C

1) FTO cleaning: the planar cell was cleaned first ultrasonically for 10 min in substrate cleaner water solution. After rinsed with deionized water, it was immersed overnight in KOH isopropyl alcohol solution (12 g/100 mL). After wash with deionized water, it was cleaned second ultrasonically in acetone and alcohol for 10 min, respectively.

2) Screen print: Colloidal DHS-TPP3 with average particle size of 20 nm (Dalian HeptaChroma SolarTech Co., Ltd) and TiO_2 film with thickness of 10.5 μm were sintered at temperature 450 °C for 30 min, and then immersed in N719 ethanol solution to sensitize for 24 hours after cooling down.

3) Cell assembly: coat electrode with a layer of 50 nm Pt by means of magnetron sputtering of FTO. 40 μm thick Slurry film (DuPont) is used as spacer. The effective area and efficiency of the cell are 0.25 cm^2 and 7.5%, respectively.

Part 4, Preparation of condenser

Preparation of a parabolic light condenser is used as an example shown in Fig. 3.

Different opening condensers are prepared by designing their opening width D and depth H. The parameters of several kinds of light condensers are p = 0.8 mm for parabolic groove, a = 20 mm and b = 6 mm for semi-elliptical groove, the bottom angle 45 degrees for V-shaped groove and glass rods of different diameter for semicircle groove.

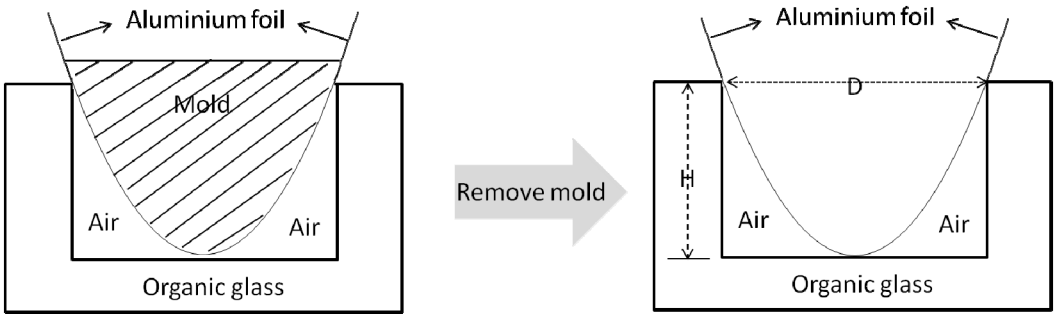

Fig. 4. Schematic of parabolic groove preparation.

Part 5, Integration of different fiber-shaped photovoltaic cell unit into panel modules

Fiber-shaped photovoltaic cells are easy to combine together into serial and parallel manner and then they are integrated into module. As showed in fig.6, there can be

one FPVC in one capillary acting as one unit to form FPVC module. Also there can be multi-FPVCs in one capillary acting as unit to be integrated into module, which is showed in Fig.7. The IV performance of three FPVCs unit module in the form showed in fig.6. and that of three FPVCs unit module in the form showed in fig.7. are summarized in Table 1. Do remember that the efficiencies are calculated using the module area not the aperture area and the test is performed under 100mW/cm_2 combined with a diffuse reflector.

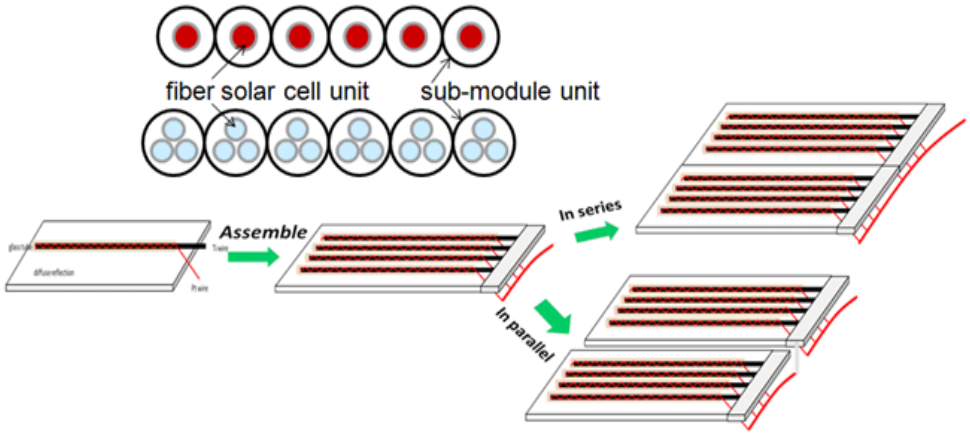

Fig.5. The scheme of fabrication solar cell module using fiber solar cells. Each fiber solar cell is placed on a diffuse board and is combined in serials or parallel using metal wire connection. The inset is the crossing of module and FDSC units. One cell in one capillary or multi-cell (e.g. three fiber solar cell units in one capillary).

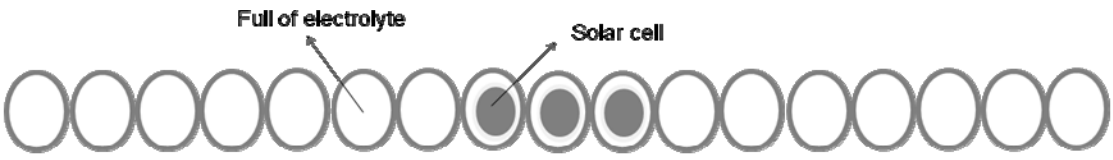

Fig.6. Cross section view of solar cell module using fiber-shaped photovoltaic cell units. The module unit is one fiber-shaped photo voltaic cell sealed in one capillary.

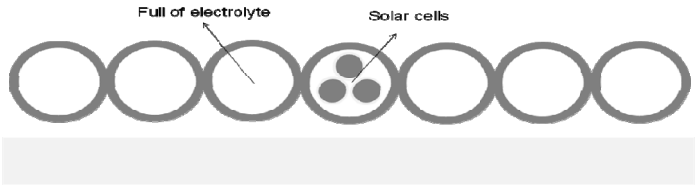

Fig. 7. Cross section view of solar cell module using fiber-shaped photovoltaic cell units. The module unit is three fiber-shaped photo-voltaic cells sealed in one capillary.

Table 1. IV performance (under AM 1.50) of Fiber-shaped photovoltaic module using different integrated solar cell units showing in fig.6 and fig.7, respectively.

	V_{oc}(V)	I_{sc}(mA/cm)	J_{sc}(mA/cm^2)	FF	PCE%
Fig.6	0.707	2.29	8.97	0.712	4.51
Fig.7	0.671	1.30	10.02	0.775	5.21